

# 1 **The rice NLR pair Pikp-1/Pikp-2 initiates cell death through** 2 **receptor cooperation rather than negative regulation**

3

4 Rafał Zdrzałek<sup>1</sup>, Sophien Kamoun<sup>2</sup>, Ryohei Terauchi<sup>3,4</sup>, Hiromasa Saitoh<sup>5\*</sup> & Mark J Banfield<sup>1\*</sup>

5

6 <sup>1</sup>Department of Biological Chemistry, John Innes Centre, Norwich Research Park, Norwich,

7 NR4 7UH, UK, <sup>2</sup>The Sainsbury Laboratory, University of East Anglia, Norwich Research Park,

8 Norwich, NR4 7UH, UK, <sup>3</sup>Division of Genomics and Breeding, Iwate Biotechnology Research

9 Centre, Iwate, Japan, <sup>4</sup>Laboratory of Crop Evolution, Graduate School of Agriculture, Kyoto

10 University, Kyoto, Japan, <sup>5</sup>Laboratory of Plant Symbiotic and Parasitic Microbes, Department

11 of Molecular Microbiology, Faculty of Life Sciences, Tokyo University of Agriculture, Tokyo

12 156-8502, Japan

13

## 14 **ORCID IDs:**

15 Rafał Zdrzałek: 0000-0003-3669-924X

16 Sophien Kamoun: 0000-0002-0290-0315

17 Ryohei Terauchi: 0000-0002-0095-4651

18 Hiromasa Saitoh: 0000-0002-0124-9276

19 Mark J Banfield: 0000-0001-8921-3835

## 20 **Abstract**

21 Plant NLR immune receptors are multidomain proteins that can function as specialized  
22 sensor/helper pairs. Paired NLR immune receptors are generally thought to function via  
23 negative regulation, where one NLR represses the activity of the second and detection of  
24 pathogen effectors relieves this repression to initiate immunity. However, whether this  
25 mechanism is common to all NLR pairs is not known. Here, we show that the rice NLR pair  
26 Pikp-1/Pikp-2, which confers resistance to strains of the blast pathogen *Magnaporthe oryzae*  
27 (*syn. Pyricularia oryzae*) expressing the AVR-PikD effector, functions via receptor cooperation,  
28 with effector-triggered activation requiring both NLRs to trigger the immune response. To  
29 investigate the mechanism of Pikp-1/Pikp-2 activation, we expressed truncated variants of  
30 these proteins, and made mutations in previously identified NLR sequence motifs. We found  
31 that any domain truncation, in either Pikp-1 or Pikp-2, prevented cell death in the presence  
32 of AVR-PikD, revealing that all domains are required for activity. Further, expression of  
33 individual Pikp-1 or Pikp-2 domains did not result in cell death. Mutations in the conserved P-  
34 loop and MHD sequence motifs in both Pikp-1 and Pikp-2 prevented cell death activation,  
35 demonstrating that these motifs are required for the function of the two partner NLRs. Finally,  
36 we showed that Pikp-1 and Pikp-2 associate to form homo- and hetero-complexes in planta  
37 in the absence of AVR-PikD; on co-expression the effector binds to Pikp-1 generating a tri-  
38 partite complex. Taken together, we provide evidence that Pikp-1 and Pikp-2 form a fine-  
39 tuned system that is activated by AVR-PikD via receptor cooperation rather than negative  
40 regulation.

## 41 **Introduction**

42 Like animals, plants are constantly threatened by pathogens and pests. To defend themselves,  
43 they have evolved a sophisticated immune system that relies on both cell surface and  
44 intracellular receptors (1, 2). The majority of cloned resistance genes are intracellular immune  
45 receptors that belong to the nucleotide-binding, leucine-rich repeat (NLR) superfamily (3).  
46 NLRs activate immunity leading to disease resistance following recognition of pathogen  
47 elicitors, typically effectors delivered into host cells to promote pathogenesis (4). NLR-  
48 mediated immunity can include localised cell death known as the Hypersensitive Response  
49 (HR) (5), which contributes to limiting pathogen spread through host tissue.

50

51 The canonical architecture of plant NLRs consists of an N-terminal Toll/Interleukin-1 receptor  
52 homology (TIR) domain or coiled-coil (CC) domain ((including the RPW8-like CC, CC<sub>R</sub>),  
53 establishing the TIR-NLR, CC-NLR and CC<sub>R</sub>-NLR families), a central NB-ARC domain  
54 (Nucleotide-binding adaptor and APAF-1, R proteins, and CED-4), and a C-terminal leucine-  
55 rich repeat (LRR) domain. Conceptual frameworks for the roles of each domain are  
56 established, although their precise role may vary from one NLR to another (6). In brief, the N-  
57 terminal TIR or CC domains are thought to be involved in triggering cell death following  
58 effector perception, with recent studies suggesting a nucleotide hydrolase activity (for TIRs  
59 (7-9)) and membrane-perturbation (for oligomeric CCs (10, 11)). The NB-ARC domain acts as  
60 a molecular switch with the conformation of the protein stabilised by the bound nucleotide,  
61 ADP or ATP (12-15). Within the NB-ARC domain, several well-conserved sequence motifs are  
62 known, with the “P-loop” and “MHD” motifs located to the nucleotide binding site (16, 17).  
63 Mutations in these motifs have diverse effects on NLR activity. For example, mutations within

64 the P-loop motif impair nucleotide binding, and often result in loss of protein function (18-  
65 20). Mutations in this motif can also prevent self-association and affect localisation (21).  
66 Mutations within the MHD motif frequently lead to constitutive activity (often called auto-  
67 activation (22-26)). The C-terminal LRR domain has a role in auto-inhibition (27-29), a function  
68 shared with animal NLRs (30-32), but can also define effector recognition specificity (33).

69

70 NLRs can function as singletons, capable of both perceiving effectors and executing a  
71 response (34, 35). This activity may require non-NLR interactors (36-40) or oligomerisation  
72 (41, 42). However, many NLRs require a second NLR for function, with three major classes  
73 described (43, 44). In each class, one of the NLRs functions as a “sensor” to detect the  
74 presence of the effector, whereas the second acts as a “helper”, and is required for cell death  
75 activity. For genetically linked sensor-helper NLR pairs, expression is driven from a shared  
76 promoter, and both proteins are required for effector perception (45). Interestingly, in many  
77 genetically linked NLR pairs, the sensor NLR contains an additional integrated domain that  
78 directly binds a pathogen effector (46-50). Integrated domains in NLRs have been found  
79 across all flowering plants (51-53). The separation of sensor/helper functions within NLR pairs  
80 may have evolutionary advantages, for example increasing tolerance to point mutations in  
81 the sensor (54).

82

83 CC-NLRs RGA5 and RGA4 from rice, and TIR-NLRs RRS1 and RPS4 from *Arabidopsis* are well  
84 established models in the study of genetically linked NLR pairs (45, 48, 55). RGA5 and RRS1  
85 are the sensor NLRs (harbouring an integrated HMA (Heavy Metal Associated) domain and  
86 integrated WRKY domain respectively), and RGA4 and RPS4 are the helpers. In both systems,  
87 the helper NLRs appear to be auto-active when expressed alone in heterologous expression

88 systems, and this auto-activity is suppressed on co-expression with the sensor NLR. Effector  
89 perception relieves suppression and initiates receptor activity (45, 56).

90

91 In rice, the CC-NLR pair Pik-1 and Pik-2 confers resistance to *Magnaporthe oryzae* (syn.  
92 *Pyricularia oryzae*) carrying the AVR-Pik effector. Similar to RGA5, Pik-1 has an integrated  
93 HMA domain, but unlike RGA5 this is positioned between the CC and NB-ARC domain, rather  
94 than after the LRR. The Pik-1 integrated HMA domain directly binds the AVR-Pik effector (50).  
95 However, how recognition of the effector translates into an immune response in the context  
96 of full-length receptors is unclear, as is the nature of any pre-activation state of the Pik-1/Pik-  
97 2 proteins. Further, which NLR domains are necessary and sufficient for immune signalling in  
98 this pair is unknown.

99 We previously showed that the AVR-Pik elicited hypersensitive cell death mediated by the Pik  
100 NLR pair can be recapitulated using transient expression in leaves of the model plant  
101 *Nicotiana benthamiana* (50, 57, 58). In this study, we investigated the roles and requirements  
102 of domains in the Pik NLR alleles Pikp-1 and Pikp-2 in planta using the *N. benthamiana*  
103 experimental system. We show that intact, full-length, Pikp-1 and Pikp-2 are necessary for a  
104 cell death response upon effector perception. Truncation of any domain results in lack of  
105 effector-dependent cell death compared to wild-type. Further, expression of any specific NLR  
106 domain, or combination of domains, does not result in cell death. We also show that native  
107 P-loop and MHD-like motifs are required in both Pikp-1 and Pikp-2 proteins for receptor  
108 activity. Finally, we demonstrate that Pikp-1 and Pikp-2 are able to form homo- and hetero-  
109 complexes in planta in the absence of the AVR-PikD. Upon binding of the AVR-PikD effector,  
110 a tri-partite complex is formed that may represent the activated state of the receptor.

## 111 **Materials and Methods**

### 112 **Cloning**

113 Domesticated sequences of full-length Pk1p-1 and Pk1p-2 (as described in (58)), and MLA10,  
114 were assembled into the pICH47751 vector under the control of the *mas* promoter and with  
115 C-terminal epitope tags (3x FLAG tag, V-5 tag or 6xHA tag accordingly) using the Golden Gate  
116 system (59). To obtain Pk1p-1 and Pk1p-2 individual domains and truncation variants, relevant  
117 sequences were amplified by PCR using the plasmids above as templates, and assembled into  
118 the pICH47751 vector under control of CaMV35S promoter and with C-terminal epitope tags  
119 (6xHis + 3xFlag (HellFire (HF)) for Pk1p-1 derivatives and 6xHA for Pk1p-2 derivatives) using the  
120 Golden Gate system. Myc:AVR-Pk1D and Myc:AVR-Pk1D<sup>H46E</sup> constructs used were as described  
121 in (58). All DNA constructs were confirmed by sequencing and transformed into  
122 *Agrobacterium tumefaciens* strain GV3101 via electroporation.

### 123 **Mutagenesis**

124 To generate Pk1p mutants (P-loop and MHD-like motifs), we introduced mutations into the  
125 relevant NB-ARC domain modules using site-directed mutagenesis. Subsequently these  
126 domain constructs were used to generate full length NLRs by assembly using the Golden Gate  
127 system. Each of the constructs were assembled with the CaMV35S promoter with relevant  
128 tags (6xHis + 3xFlag (HellFire (HF)) for Pk1p-1 derivatives and 6xHA tag for Pk1p-2 derivatives).

### 129 **Cell death assays**

130 *Agrobacterium tumefaciens* strain GV3101 carrying the appropriate constructs were  
131 suspended in infiltration buffer (10 mM MgCl<sub>2</sub>, 10 mM MES, pH 5.6, 150 mM acetosyringone)  
132 and mixed prior to infiltration at the following final OD<sub>600</sub>: NLRs and NLR-derivatives 0.4,

133 effectors 0.6, P19 (silencing suppressor) 0.1. Bacteria were infiltrated into leaves of ~4 weeks  
134 old *N. benthamiana* plants using a 1ml needleless syringe. At 5 days post infiltration (dpi),  
135 detached leaves were imaged under UV light on the abaxial side, and visually scored for cell  
136 death response (see below). To confirm protein expression, representative infiltration spots  
137 were prepared, frozen in liquid nitrogen, ground to a fine powder, mixed with extraction  
138 buffer (see below) in 2 ml/g ratio, centrifuged, mixed with loading dye and loaded on an SDS-  
139 PAGE gel for western blot analysis.

## 140 **Cell death scoring**

141 Pictures of the leaves at 5 dpi were taken as described previously (57) and cell death (visible  
142 as green fluorescence area under the UV light) was scored according to the scale presented  
143 in (50). The dot plots were generated using R v3.4.3 (<https://www.r-project.org/>) and the  
144 graphic package ggplot2 (60). Dots represent the individual datapoints and the size of larger  
145 circles is proportional to the number of dots within that score. Dots of the same colour within  
146 one plot come from the same biological repeat. All positive and negative controls were also  
147 scored and are represented on relevant plots. As positive and negative controls were included  
148 on most leaves there are more data points for these samples.

## 149 **Co-Immunoprecipitation**

150 Protein extraction was conducted as described in (61) with minor modifications. Extraction  
151 buffer GTEN (10% glycerol, 25 mM Tris, pH 7.5, 1 mM EDTA, 150 mM NaCl), 2% w/v PVPP, 10  
152 mM DTT, 1× protease inhibitor cocktail (Sigma), 0.1% Tween 20 (Sigma) was added to frozen  
153 tissue in 2 ml/g ratio. The sample was resuspended and centrifuged for 30 min (4500g) at 4°C.  
154 The supernatant was filtered through a 0.45 µm filter. Anti-FLAG M2 magnetic beads (Sigma,  
155 M8823) were washed with the IP buffer (GTEN + 0.1% Tween 20), resuspended, and added to

156 protein extracts (20  $\mu$ l of resin per 1.5 ml of extract). Samples were incubated for an hour at  
157 4°C with gentle shaking. Following incubation, the resin was separated using magnetic stand  
158 and washed 5 times with IP buffer. For elution, beads were mixed with 30  $\mu$ l of Loading Dye  
159 and incubated at 70°C for 10 min. Finally, samples were centrifuged and loaded on a precast  
160 gradient gel (4-20%, Expedeon) for western blot analysis.

## 161 **Western blot**

162 Western blots were performed as described previously (61). Following SDS-PAGE, proteins  
163 were transferred onto PVDF membrane using Trans-Blot Turbo Transfer Kit (Biorad) and  
164 blocked in 5% milk in TBS-T (50mM Tris-HCl, 150mM NaCl, 0.1% Tween20, pH 8.0) at 4°C for  
165 at least 1 hour. Respective primary HRP-conjugated antibodies ( $\alpha$ -FLAG: Cohesion  
166 Biosciences, CPA9020;  $\alpha$ -HA: Invitrogen, #26183-HRP;  $\alpha$ -V-5: Invitrogen, #MA5-15253-HRP;  
167  $\alpha$ -Myc (9E10): Santa Cruz Biotechnology, SC-40) were applied for overnight incubation (4°C).  
168 Membranes were then rinsed with TBS-T. Proteins were detected using ECL Extreme reagents  
169 (Expedeon) in chemiluminescence CCD camera (ImageQuant LAS 500).



## 170 **Results**

### 171 **Each domain of Pikp-1 and Pikp-2 is required for receptor activation**

172 To investigate the roles and requirements for individual domains of Pikp-1 (CC, HMA, NB-ARC  
173 and LRR) and Pikp-2 (CC, NB-ARC and LRR) in triggering cell death, we transiently expressed  
174 each of these in *N. benthamiana* using *Agrobacterium tumefaciens* mediated transformation  
175 (henceforth agroinfiltration). All constructs were tagged at their C-terminus with the HellFire  
176 tag (6xHis + 3xFlag (HF), for Pikp-1 domains) or HA tag (for Pikp-2 domains). The boundaries  
177 of the domains used were as defined in (50).

178

179 We found that each of the individual domains of either Pikp-1 or Pikp-2 were unable to trigger  
180 cell death when expressed alone, or in the presence of the corresponding paired NLR and/or  
181 effector (Fig 1, Fig 2, S1 Fig). We confirmed that all the proteins accumulated to detectable  
182 levels using western blot analysis (S2 Fig). We then systematically truncated Pikp-1 or Pikp-2  
183 at relevant domain boundaries, and expressed these alone or in the presence of the  
184 corresponding paired NLR and/or effector, to search for any minimum functional unit (Fig 1B,  
185 Fig 2A, Fig 2B, S1 Fig). In all cases tested no cell death was observed, despite the proteins  
186 accumulating in plant tissues (S2 Fig). The only combination that gave cell death was the  
187 positive control of full length Pikp-1 and Pikp-2 in the presence of AVR-PikD. These results  
188 show that the Pikp-1/Pikp-2 pair work together to deliver a cell death response on effector  
189 perception, and all domains are required for activity.

## 190 **Conserved NB-ARC domain sequence motifs are required for Pikp-1** 191 **and Pikp-2 activity**

192 Next, we tested whether previously characterised sequence motifs within the nucleotide-  
193 binding pocket of the Pikp-1 and Pikp-2 NB-ARC domains are required for receptor activity.  
194 Firstly, we generated mutations in the P-loop motifs of Pikp-1 and Pikp-2 (Pikp-1<sup>K296R</sup> and Pikp-  
195 2<sup>K217R</sup>). Such mutations restrict nucleotide binding, and have previously been shown to impair  
196 NLR function (18, 19, 62, 63). On expression in *N. benthamiana* via agroinfiltration, we found  
197 that these mutations abolish cell death activity in planta, including when expressed in the  
198 presence of the paired NLR and the AVR-PikD effector (Fig 3, S3A Fig). This reveals that an  
199 intact P-loop motif is required in both Pikp-1 and Pikp-2 for activity. Expression of all proteins  
200 was confirmed by western blot analysis (S3B Fig). Secondly, we generated mutations in the  
201 “MHD” motifs of Pikp-1 and Pikp-2. Although classically defined as Methionine-Histidine-  
202 Aspartate (MHD), the residues that comprise this motif in plant NLRs can vary. Here we will  
203 refer to this as the MHD-like motif. In Pikp-1, the MHD-like motif residues are Ile-His-Pro (IHP),  
204 while in Pikp-2 they are Val-His-Asp (VHD). Mutations within this NLR motif frequently lead to  
205 auto-activation and cell death in the absence of pathogen perception (64-66). To determine  
206 the importance of the MHD-like motif for Pikp-1 and Pikp-2 activity, we generated triple  
207 alanine mutants of each protein (Pikp-1<sup>599IHP601→AAA</sup>, and Pikp-2<sup>557VHD559→AAA</sup>) and a Pikp-2<sup>D559V</sup>  
208 mutant. On expression in *N. benthamiana* via agroinfiltration, we found that expression of  
209 these mutants alone did not result in auto-activity and cell death (Fig 3). We also found that  
210 any combination of the MHD-like motif mutants with wild-type or mutant paired NLRs, with  
211 or without the AVR-PikD effector, did not result in cell death (Fig 3B, Fig 3D). These results  
212 show that the native MHD-like motifs of Pikp-1 and Pikp-2 are required to trigger cell death.

213 All proteins were expressed to detectable levels, as confirmed by western blot analysis (S3B  
214 Fig).

215

## 216 **Pikp-1 and Pikp-2 form homo- and hetero-complexes in planta**

217 Paired NLRs can form homo- and hetero-complexes in planta (45, 48). To investigate whether  
218 Pikp-1 and Pikp-2 can also homo- and/or hetero-associate, both in the absence and in the  
219 presence of the effector, we performed in planta co-immunoprecipitation (co-IP) assays. To  
220 test for homo-complex formation we expressed differentially tagged Pikp-1 constructs (FLAG  
221 tag and V-5 tag), or Pikp-2 constructs (FLAG tag and HA tag) in *N. benthamiana* via  
222 agroinfiltration, followed by immunoprecipitation with  $\alpha$ -FLAG resin. The barley NLR MLA10  
223 (expressed with a FLAG tag) served as a negative control for interactions. Each FLAG-tagged  
224 protein was expressed, and immunoprecipitated as expected (lower panels, Fig 4A, Fig 4B).  
225 For Pikp-1, we observe co-immunoprecipitation of Pikp-1:V-5 with Pikp-1:FLAG, but not with  
226 MLA10:FLAG, and Pikp-1:V-5 did not show non-specific interaction with the resin when  
227 expressed alone (Fig 4A). Similar results were obtained for Pikp-2 (Fig 4B), where Pikp-2:HA  
228 immunoprecipitated Pikp-2:FLAG on co-expression. Faint bands of Pikp-2:HA were also  
229 observed with MLA10:FLAG. However, a similar band can be observed where Pikp-2:HA is  
230 expressed alone, indicating a weak non-specific binding to the resin. The presence of the AVR-  
231 PikD effector (or the mutant AVR-PikD<sup>H46E</sup> as a negative control) does not affect the homo-  
232 association of Pikp-1 or Pikp-2 (S4 Fig).

233

234 We then tested whether Pikp-1 and Pikp-2 can form hetero-complexes. Using the resources  
235 described above, we co-expressed the proteins and performed  $\alpha$ -FLAG pull downs. We show

236 that Pknp-2:HA co-immunoprecipitated with Pknp-1:FLAG, but not with MLA10:FLAG,  
237 indicating that these NLRs specifically hetero-associate (Fig 5A). We also tested whether co-  
238 expression with AVR-PknpD affects the formation of Pknp-1/Pknp-2 hetero-complexes. We co-  
239 expressed Pknp-1:V-5, Pknp-2:FLAG and Myc:AVR-PknpD followed by  $\alpha$ -FLAG pull down (note: in  
240 this case Pknp-2:FLAG is immunoprecipitated). All three proteins could be detected after  $\alpha$ -  
241 FLAG pull down (Fig 5B). We suggest that Pknp-2 associates with Pknp-1, which is also bound  
242 to the AVR-PknpD effector, forming tri-partite complex. Co-expression with the AVR-PknpD<sup>H46E</sup>  
243 mutant was used as a negative control for effector interaction.

## 244 Discussion

245 Genetically linked NLR pairs are emerging as an important class of immune receptor in plants.  
246 Established models for paired NLR receptors suggest they function via negative regulation  
247 where a sensor NLR, that often carries an integrated domain, represses the activity of the  
248 second. Binding of pathogen effectors to the sensor NLR relieves this negative regulation. In  
249 this study, we show that the rice NLR pair Pikp-1/Pikp-2 differs from this model and works via  
250 receptor cooperation. Pikp-2 is not auto-active when expressed in the absence of Pikp-1. Both  
251 Pikp-1 and Pikp-2 are required to trigger cell death upon binding of the AVR-PikD effector to  
252 the integrated HMA domain of Pikp-1, and all the domains are indispensable for this activity.  
253 Further, we determined the requirements for conserved NB-ARC domain sequence motifs,  
254 the P-loop and MHD-like motifs. Finally, we find Pikp-1 and Pikp-2 can form homo- and  
255 hetero-complexes that are likely important for function.

256

257 The expression of individual domains of a number of NLRs can result in cell death. In  
258 particular, CC domains and other N-terminal truncations can induce cell death when  
259 expressed in planta (19, 42, 67-70). This is thought to reflect oligomerization of the CC  
260 domains, resulting in minimal functional units that can trigger cell death. However, the CC  
261 domains of either Pikp-1 or Pikp-2 did not display cell death inducing activity. This likely  
262 reflects an inability of these domains to adopt a configuration that supports cell death when  
263 expressed alone. Further, we did not observe cell death on expression of full-length Pikp-1  
264 with the Pikp-2 CC domain (with or without AVR-PikD). We consider this a biologically relevant  
265 test for CC domain-mediated cell death in a paired NLR compared to co-expression of the CC  
266 domains with short epitope tags, or fused to GFP/YFP (a strategy required to observe cell

267 death for some CC domains (38, 39, 71), but not used here). It is possible that further studies  
268 may identify a Pikip-1 or Pikip-2 CC domain construct that supports cell death, as studies with  
269 MLA10 family NLRs showed that a single amino acid change can make the difference between  
270 observing cell death or not (69), and chimeric NLRs with swaps within the CC domains can  
271 result in cell death (72).

272

273 Considering NLR regions other than the N-terminal domains, expression of the NB-ARC from  
274 Rx resulted in cell death (73). However, we did not observe this phenotype on expression of  
275 the NB-ARC domains of Pikip1 or Pikip-2. For the NLR RPS5, it was shown that a CC-NB-ARC  
276 construct can elicit cell death (40), but this may be due to deletion of the LRR domain that  
277 may have a role in auto-inhibition prior to effector detection (28). We did not observe cell  
278 death following deletion of the LRR domains of Pikip-1 or Pikip-2. Together, our data shows  
279 that full-length Pikip proteins, and perception of the effector, are required for cell death  
280 activity in planta. This is an effective strategy to prevent mis-regulation of receptor activity in  
281 the absence of the pathogen, but highlights the need for additional studies to understand the  
282 molecular mechanistic basis of Pikip activation, and the diversity of paired NLR function more  
283 generally.

284

285 Although the P-loop motif is required for NLRs reported to work as singletons (18, 20), it is  
286 not always necessary for paired and networked NLRs (45, 56, 74). In genetically linked pairs  
287 RGA5/RGA4 and RRS1/RPS4, the helper NLR requires an intact P-loop for cell death, but not  
288 the sensor (45, 56). In CC<sub>R</sub>-type helper NLRs, such as ADR1 and NRG1 (which function  
289 downstream of several other NLRs, but are not genetically linked (75)), an intact P-loop motif  
290 may not be required (76, 77). Pikip-1 and Pikip-2 appear to function similar to the NRC network

291 of solanaceous plants, where both sensor and helper NLRs require a native P-loop motif for  
292 function (74). So why do Pikp-1 and Pikp-2 both require a native P-loop? It maybe this just  
293 provides an additional layer of regulation. It is also possible that mutations in the P-loop affect  
294 protein folding by preventing ADP binding, and Pikp-1 is more sensitive to this than other  
295 sensor NLRs studied, or that ADP/ATP exchange is more important for transducing effector  
296 binding by the HMA integrated domain in Pikp-1, possibly determined by the unusual position  
297 of the integrated domain between the CC and NB-ARC domain in this NLR.

298

299 Residues of the MHD-like motif are involved in binding ADP in the inactive state of NLRs (12,  
300 78), and mutations in this motif can lead to auto-activity (22, 23). Mutations in the MHD-like  
301 motif of Pikp-1 and Pikp-2 are not auto-active, and result in a loss of cell death activity when  
302 expressed with the AVR-PikD effector. In RGA5 and RGA4, residues of the MHD-like motif are  
303 LHH and TYG, respectively, and the presence of a Glycine (G) in the third position of RGA4 was  
304 shown to be linked to RGA4 auto-activity, whereas introducing mutations into MHD-like motif  
305 of RGA5 did not abolish its ability to repress RGA4 (45). The most straightforward explanation  
306 for why changes at the MHD-like motif in Pikp-1 and Pikp-2 results in a loss of any cell death  
307 activity, rather than autoactivation, is that these mutations do not support the protein  
308 confirmation required, perhaps in the context of this NLR pair specifically.

309

310 Plant NLRs can form both homo- and hetero-complexes both prior to and after effector  
311 recognition (21, 40, 42, 79, 80), or undergo effector induced oligomerisation (81). In addition  
312 to the CC domains of CC-NLRs, the N-terminal TIR domains of TIR-NLRs have been shown to  
313 oligomerise (82-84). Recently, the structure of full-length ZAR1 revealed the role of  
314 oligomerisation in activation of a full-length NLR (11). Here, we have shown that Pikp-1 and

315 Pknp-2 form both homo- and hetero-complexes in the absence and presence of the AVR-PknpD  
316 effector. However, the conformation of the proteins, their stoichiometry, and their specific  
317 arrangement within the complexes, remain to be determined. Various models are possible  
318 for the active complex including a Pknp-1/Pknp-2 dimer, a higher order oligomer including  
319 multiple copies of the dimer, or a structure where Pknp-1 initiates the oligomerisation of Pknp-  
320 2 similar to the mechanism seen for NAIP2/NLRC4 (85) and NAIP5/NLRC4 (86).

321

322 In summary, our findings reveal that the Pknp-1/Pknp-2 NLR pair function via receptor  
323 cooperation rather than a suppression/activation mechanism, and signalling in planta  
324 requires the full-length proteins with native sequences at the P-loop and MHD-like sequence  
325 motifs. This suggests multiple mechanisms of regulation exist for NLRs. It is important to  
326 further investigate these mechanisms if we are to fully understand NLR function and use this  
327 to engineer improved disease resistance phenotypes in crops.



## 328 **Acknowledgements**

329 This work was supported by the UKRI Biotechnology and Biological Sciences Research  
330 Council (BBSRC) Norwich Research Park Biosciences Doctoral Training Partnership, UK [grant  
331 BB/M011216/1]; the UKRI BBSRC, UK [grants BB/P012574, BB/M02198X]; the European  
332 Research Council [ERC; proposal 743165]; the John Innes Foundation; the Japan Society for  
333 the Promotion of Science (JSPS KAKENHI; proposal 18K05657, 15H05779, and 20H00421), and  
334 by the Strategic Research Project from Tokyo University of Agriculture. We thank Juan Carlos  
335 De la Concepcion and Josephine Maidment for help with cloning. We also thank Thorsten  
336 Langner and Hiroaki Adachi for comments on the manuscript.

## 337 **References**

- 338 1. Cesari S. Multiple strategies for pathogen perception by plant immune receptors. *New Phytol.*  
339 2017.
- 340 2. Couto D, Zipfel C. Regulation of pattern recognition receptor signalling in plants. *Nat Rev*  
341 *Immunol.* 2016;16(9):537-52.
- 342 3. Kourelis J, van der Hoorn RAL. Defended to the Nines: 25 Years of Resistance Gene Cloning  
343 Identifies Nine Mechanisms for R Protein Function. *Plant Cell.* 2018;30(2):285-99.
- 344 4. El Kasmi F, Horvath D, Lahaye T. Microbial effectors and the role of water and sugar in the  
345 infection battle ground. *Curr Opin Plant Biol.* 2018;44:98-107.
- 346 5. Dodds PN, Rathjen JP. Plant immunity: towards an integrated view of plant-pathogen  
347 interactions. *Nat Rev Genet.* 2010;11(8):539-48.
- 348 6. Sukarta OCA, Sloomweg EJ, Govers A. Structure-informed insights for NLR functioning in plant  
349 immunity. *Semin Cell Dev Biol.* 2016;56:134-49.
- 350 7. Horsefield S, Burdett H, Zhang X, Manik MK, Shi Y, Chen J, et al. NAD(+) cleavage activity by  
351 animal and plant TIR domains in cell death pathways. *Science.* 2019;365(6455):793-9.
- 352 8. Wan L, Essuman K, Anderson RG, Sasaki Y, Monteiro F, Chung EH, et al. TIR domains of plant  
353 immune receptors are NAD(+)-cleaving enzymes that promote cell death. *Science.*  
354 2019;365(6455):799-803.
- 355 9. Essuman K, Summers DW, Sasaki Y, Mao X, Yim AKY, DiAntonio A, et al. TIR Domain Proteins  
356 Are an Ancient Family of NAD(+)-Consuming Enzymes. *Curr Biol.* 2018;28(3):421-30 e4.
- 357 10. Burdett H, Bentham AR, Williams SJ, Dodds PN, Anderson PA, Banfield MJ, et al. The Plant  
358 "Resistosome": Structural Insights into Immune Signaling. *Cell Host Microbe.* 2019;26(2):193-201.
- 359 11. Wang J, Hu M, Wang J, Qi J, Han Z, Wang G, et al. Reconstitution and structure of a plant NLR  
360 resistosome conferring immunity. *Science.* 2019;364(6435).
- 361 12. Wang J, Wang J, Hu M, Wu S, Qi J, Wang G, et al. Ligand-triggered allosteric ADP release primes  
362 a plant NLR complex. *Science.* 2019;364(6435).
- 363 13. Zhang X, Dodds PN, Bernoux M. What Do We Know About NOD-Like Receptors in Plant  
364 Immunity? *Annu Rev Phytopathol.* 2017;55:205-29.
- 365 14. Bernoux M, Burdett H, Williams SJ, Zhang X, Chen C, Newell K, et al. Comparative Analysis of  
366 the Flax Immune Receptors L6 and L7 Suggests an Equilibrium-Based Switch Activation Model. *Plant*  
367 *Cell.* 2016;28(1):146-59.
- 368 15. Tameling WI, Vossen JH, Albrecht M, Lengauer T, Berden JA, Haring MA, et al. Mutations in  
369 the NB-ARC domain of I-2 that impair ATP hydrolysis cause autoactivation. *Plant Physiol.*  
370 2006;140(4):1233-45.
- 371 16. Albrecht M, Takken FL. Update on the domain architectures of NLRs and R proteins. *Biochem*  
372 *Biophys Res Commun.* 2006;339(2):459-62.
- 373 17. Meyers BC, Dickerman AW, Michelmore RW, Sivaramakrishnan S, Sobral BW, Young ND. Plant  
374 disease resistance genes encode members of an ancient and diverse protein family within the  
375 nucleotide-binding superfamily. *Plant J.* 1999;20(3):317-32.
- 376 18. Bai S, Liu J, Chang C, Zhang L, Maekawa T, Wang Q, et al. Structure-function analysis of barley  
377 NLR immune receptor MLA10 reveals its cell compartment specific activity in cell death and disease  
378 resistance. *PLoS Pathog.* 2012;8(6):e1002752.
- 379 19. Howles P, Lawrence G, Finnegan J, McFadden H, Ayliffe M, Dodds P, et al. Autoactive alleles  
380 of the flax L6 rust resistance gene induce non-race-specific rust resistance associated with the  
381 hypersensitive response. *Mol Plant Microbe Interact.* 2005;18(6):570-82.
- 382 20. Dinesh-Kumar SP, Tham WH, Baker BJ. Structure-function analysis of the tobacco mosaic virus  
383 resistance gene N. *Proc Natl Acad Sci U S A.* 2000;97(26):14789-94.

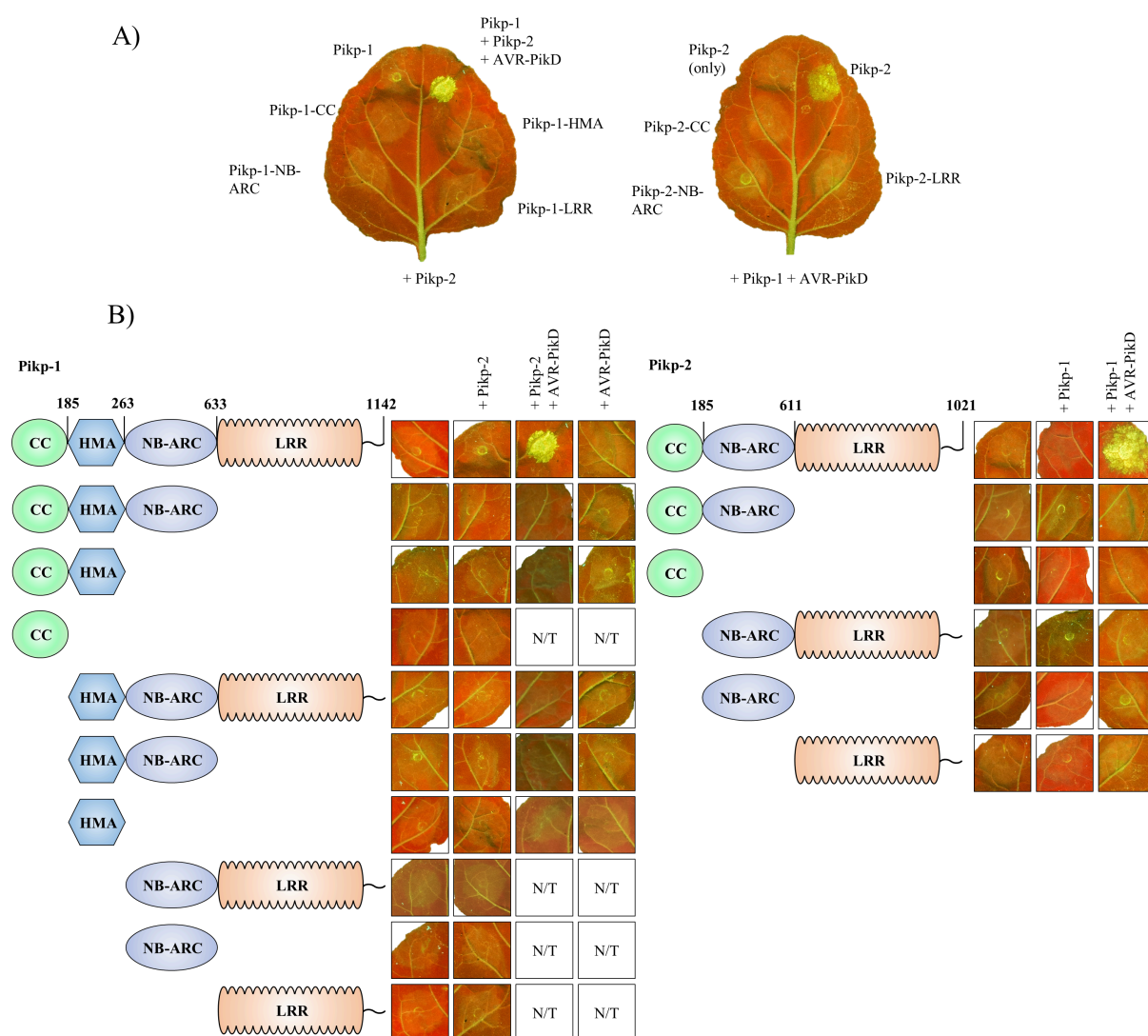
- 384 21. El Kasmi F, Chung EH, Anderson RG, Li J, Wan L, Eitas TK, et al. Signaling from the plasma-  
385 membrane localized plant immune receptor RPM1 requires self-association of the full-length protein.  
386 *Proc Natl Acad Sci U S A*. 2017;114(35):E7385-E94.
- 387 22. Li J, Huang H, Zhu M, Huang S, Zhang W, Dinesh-Kumar SP, et al. A Plant Immune Receptor  
388 Adopts a Two-Step Recognition Mechanism to Enhance Viral Effector Perception. *Mol Plant*.  
389 2019;12(2):248-62.
- 390 23. Roberts M, Tang S, Stallmann A, Dangl JL, Bonardi V. Genetic requirements for signaling from  
391 an autoactive plant NB-LRR intracellular innate immune receptor. *PLoS Genet*. 2013;9(4):e1003465.
- 392 24. Gao Z, Chung EH, Eitas TK, Dangl JL. Plant intracellular innate immune receptor Resistance to  
393 *Pseudomonas syringae* pv. *maculicola* 1 (RPM1) is activated at, and functions on, the plasma  
394 membrane. *Proc Natl Acad Sci U S A*. 2011;108(18):7619-24.
- 395 25. Kawano Y, Akamatsu A, Hayashi K, Housen Y, Okuda J, Yao A, et al. Activation of a Rac GTPase  
396 by the NLR family disease resistance protein Pit plays a critical role in rice innate immunity. *Cell Host*  
397 *Microbe*. 2010;7(5):362-75.
- 398 26. Bendahmane A, Farnham G, Moffett P, Baulcombe DC. Constitutive gain-of-function mutants  
399 in a nucleotide binding site-leucine rich repeat protein encoded at the Rx locus of potato. *Plant J*.  
400 2002;32(2):195-204.
- 401 27. Slootweg EJ, Spiridon LN, Roosien J, Butterbach P, Pomp R, Westerhof L, et al. Structural  
402 determinants at the interface of the ARC2 and leucine-rich repeat domains control the activation of  
403 the plant immune receptors Rx1 and Gpa2. *Plant Physiol*. 2013;162(3):1510-28.
- 404 28. Qi D, DeYoung BJ, Innes RW. Structure-function analysis of the coiled-coil and leucine-rich  
405 repeat domains of the RPS5 disease resistance protein. *Plant Physiol*. 2012;158(4):1819-32.
- 406 29. Rairdan GJ, Moffett P. Distinct domains in the ARC region of the potato resistance protein Rx  
407 mediate LRR binding and inhibition of activation. *Plant Cell*. 2006;18(8):2082-93.
- 408 30. Burdett H, Kobe B, Anderson PA. Animal NLRs continue to inform plant NLR structure and  
409 function. *Arch Biochem Biophys*. 2019;670:58-68.
- 410 31. Bentham A, Burdett H, Anderson PA, Williams SJ, Kobe B. Animal NLRs provide structural  
411 insights into plant NLR function. *Ann Bot*. 2017;119(5):827-702.
- 412 32. Hu Z, Zhou Q, Zhang C, Fan S, Cheng W, Zhao Y, et al. Structural and biochemical basis for  
413 induced self-propagation of NLRC4. *Science*. 2015;350(6259):399-404.
- 414 33. Jia Y, McAdams SA, Bryan GT, Hershey HP, Valent B. Direct interaction of resistance gene and  
415 avirulence gene products confers rice blast resistance. *EMBO J*. 2000;19(15):4004-14.
- 416 34. Adachi H, Derevnina L, Kamoun S. NLR singletons, pairs, and networks: evolution, assembly,  
417 and regulation of the intracellular immunoreceptor circuitry of plants. *Curr Opin Plant Biol*.  
418 2019;50:121-31.
- 419 35. Cesari S, Moore J, Chen C, Webb D, Periyannan S, Mago R, et al. Cytosolic activation of cell  
420 death and stem rust resistance by cereal MLA-family CC-NLR proteins. *Proc Natl Acad Sci U S A*.  
421 2016;113(36):10204-9.
- 422 36. Townsend PD, Dixon CH, Slootweg EJ, Sukarta OCA, Yang AWH, Hughes TR, et al. The  
423 intracellular immune receptor Rx1 regulates the DNA-binding activity of a Golden2-like transcription  
424 factor. *J Biol Chem*. 2018;293(9):3218-33.
- 425 37. Leibman-Markus M, Pizarro L, Schuster S, Lin ZJD, Gershony O, Bar M, et al. The intracellular  
426 nucleotide-binding leucine-rich repeat receptor (SINRC4a) enhances immune signalling elicited by  
427 extracellular perception. *Plant Cell Environ*. 2018;41(10):2313-27.
- 428 38. Baudin M, Hassan JA, Schreiber KJ, Lewis JD. Analysis of the ZAR1 Immune Complex Reveals  
429 Determinants for Immunity and Molecular Interactions. *Plant Physiol*. 2017;174(4):2038-53.
- 430 39. Hamel LP, Sekine KT, Wallon T, Sugiwaka Y, Kobayashi K, Moffett P. The Chloroplastic Protein  
431 THF1 Interacts with the Coiled-Coil Domain of the Disease Resistance Protein N' and Regulates Light-  
432 Dependent Cell Death. *Plant Physiol*. 2016;171(1):658-74.
- 433 40. Ade J, DeYoung BJ, Golstein C, Innes RW. Indirect activation of a plant nucleotide binding site-  
434 leucine-rich repeat protein by a bacterial protease. *Proc Natl Acad Sci U S A*. 2007;104(7):2531-6.

- 435 41. Saur IM, Conlan BF, Rathjen JP. The N-terminal domain of the tomato immune protein Prf  
436 contains multiple homotypic and Pto kinase interaction sites. *J Biol Chem*. 2015;290(18):11258-67.
- 437 42. Wang GF, Ji J, El-Kasmi F, Dangl JL, Johal G, Balint-Kurti PJ. Molecular and functional analyses  
438 of a maize autoactive NB-LRR protein identify precise structural requirements for activity. *PLoS*  
439 *Pathog*. 2015;11(2):e1004674.
- 440 43. Jubic LM, Saile S, Furzer OJ, El Kasmi F, Dangl JL. Help wanted: helper NLRs and plant immune  
441 responses. *Curr Opin Plant Biol*. 2019;50:82-94.
- 442 44. Wu CH, Derevnina L, Kamoun S. Receptor networks underpin plant immunity. *Science*.  
443 2018;360(6395):1300-1.
- 444 45. Cesari S, Kanzaki H, Fujiwara T, Bernoux M, Chalvon V, Kawano Y, et al. The NB-LRR proteins  
445 RGA4 and RGA5 interact functionally and physically to confer disease resistance. *EMBO J*.  
446 2014;33(17):1941-59.
- 447 46. Guo L, Cesari S, de Guillen K, Chalvon V, Mammri L, Ma M, et al. Specific recognition of two  
448 MAX effectors by integrated HMA domains in plant immune receptors involves distinct binding  
449 surfaces. *Proc Natl Acad Sci U S A*. 2018;115(45):11637-42.
- 450 47. Ortiz D, de Guillen K, Cesari S, Chalvon V, Gracy J, Padilla A, et al. Recognition of the  
451 Magnaporthe oryzae Effector AVR-Pia by the Decoy Domain of the Rice NLR Immune Receptor RGA5.  
452 *Plant Cell*. 2017;29(1):156-68.
- 453 48. Huh SU, Cevik V, Ding P, Duxbury Z, Ma Y, Tomlinson L, et al. Protein-protein interactions in  
454 the RPS4/RRS1 immune receptor complex. *PLoS Pathog*. 2017;13(5):e1006376.
- 455 49. Zhang ZM, Ma KW, Gao L, Hu Z, Schwizer S, Ma W, et al. Mechanism of host substrate  
456 acetylation by a YopJ family effector. *Nat Plants*. 2017;3:17115.
- 457 50. Maqbool A, Saitoh H, Franceschetti M, Stevenson CE, Uemura A, Kanzaki H, et al. Structural  
458 basis of pathogen recognition by an integrated HMA domain in a plant NLR immune receptor. *Elife*.  
459 2015;4.
- 460 51. Kroj T, Chanclud E, Michel-Romiti C, Grand X, Morel JB. Integration of decoy domains derived  
461 from protein targets of pathogen effectors into plant immune receptors is widespread. *New Phytol*.  
462 2016;210(2):618-26.
- 463 52. Sarris PF, Cevik V, Dagdas G, Jones JD, Krasileva KV. Comparative analysis of plant immune  
464 receptor architectures uncovers host proteins likely targeted by pathogens. *BMC Biol*. 2016;14:8.
- 465 53. Cesari S, Bernoux M, Moncuquet P, Kroj T, Dodds PN. A novel conserved mechanism for plant  
466 NLR protein pairs: the "integrated decoy" hypothesis. *Front Plant Sci*. 2014;5:606.
- 467 54. Baggs E, Dagdas G, Krasileva KV. NLR diversity, helpers and integrated domains: making sense  
468 of the NLR IDentity. *Curr Opin Plant Biol*. 2017;38:59-67.
- 469 55. Ma Y, Guo H, Hu L, Martinez PP, Moschou PN, Cevik V, et al. Distinct modes of derepression  
470 of an Arabidopsis immune receptor complex by two different bacterial effectors. *Proc Natl Acad Sci U*  
471 *S A*. 2018;115(41):10218-27.
- 472 56. Williams SJ, Sohn KH, Wan L, Bernoux M, Sarris PF, Segonzac C, et al. Structural basis for  
473 assembly and function of a heterodimeric plant immune receptor. *Science*. 2014;344(6181):299-303.
- 474 57. De la Concepcion JC, Franceschetti M, MacLean D, Terauchi R, Kamoun S, Banfield MJ. Protein  
475 engineering expands the effector recognition profile of a rice NLR immune receptor. *Elife*. 2019;8.
- 476 58. De la Concepcion JC, Franceschetti M, Maqbool A, Saitoh H, Terauchi R, Kamoun S, et al.  
477 Polymorphic residues in rice NLRs expand binding and response to effectors of the blast pathogen.  
478 *Nat Plants*. 2018;4(8):576-85.
- 479 59. Engler C, Kandzia R, Marillonnet S. A one pot, one step, precision cloning method with high  
480 throughput capability. *PLoS One*. 2008;3(11):e3647.
- 481 60. Wickham H. *ggplot2: Elegant Graphics for Data Analysis*. Springer-Verlag New York. 2016.
- 482 61. Win J, Kamoun S, Jones AM. Purification of effector-target protein complexes via transient  
483 expression in *Nicotiana benthamiana*. *Methods Mol Biol*. 2011;712:181-94.

- 484 62. Williams SJ, Sornaraj P, deCourcy-Ireland E, Menz RI, Kobe B, Ellis JG, et al. An autoactive  
485 mutant of the M flax rust resistance protein has a preference for binding ATP, whereas wild-type M  
486 protein binds ADP. *Mol Plant Microbe Interact.* 2011;24(8):897-906.
- 487 63. Tameling WIL, Elzinga SDJ, Darmin PS, Vossen JH, Takken FLW, Haring MA, et al. The Tomato  
488 R Gene Products I-2 and Mi-1 Are Functional ATP Binding Proteins with ATPase Activity. *The Plant Cell.*  
489 2002;14(11):2929-39.
- 490 64. Takken FL, Goverse A. How to build a pathogen detector: structural basis of NB-LRR function.  
491 *Curr Opin Plant Biol.* 2012;15(4):375-84.
- 492 65. van Ooijen G, Mayr G, Kasiem MM, Albrecht M, Cornelissen BJ, Takken FL. Structure-function  
493 analysis of the NB-ARC domain of plant disease resistance proteins. *J Exp Bot.* 2008;59(6):1383-97.
- 494 66. de la Fuente van Bentem S, Vossen JH, de Vries KJ, van Wees S, Tameling WI, Dekker HL, et al.  
495 Heat shock protein 90 and its co-chaperone protein phosphatase 5 interact with distinct regions of  
496 the tomato I-2 disease resistance protein. *Plant J.* 2005;43(2):284-98.
- 497 67. Lee H-Y, Mang H, Choi E-H, Seo Y-E, Kim M-S, Oh S, et al. Genome-wide functional analysis of  
498 hot pepper immune receptors reveals an autonomous NLR cluster in seed plants. *bioRxiv.*  
499 2020:2019.12.16.878959.
- 500 68. Wroblewski T, Spiridon L, Martin EC, Petrescu AJ, Cavanaugh K, Truco MJ, et al. Genome-wide  
501 functional analyses of plant coiled-coil NLR-type pathogen receptors reveal essential roles of their N-  
502 terminal domain in oligomerization, networking, and immunity. *PLoS Biol.* 2018;16(12):e2005821.
- 503 69. Casey LW, Lavrencic P, Bentham AR, Cesari S, Ericsson DJ, Croll T, et al. The CC domain  
504 structure from the wheat stem rust resistance protein Sr33 challenges paradigms for dimerization in  
505 plant NLR proteins. *Proc Natl Acad Sci U S A.* 2016.
- 506 70. Maekawa T, Cheng W, Spiridon LN, Toller A, Lukasik E, Saijo Y, et al. Coiled-coil domain-  
507 dependent homodimerization of intracellular barley immune receptors defines a minimal functional  
508 module for triggering cell death. *Cell Host Microbe.* 2011;9(3):187-99.
- 509 71. Krasileva KV, Dahlbeck D, Staskawicz BJ. Activation of an Arabidopsis resistance protein is  
510 specified by the in planta association of its leucine-rich repeat domain with the cognate oomycete  
511 effector. *Plant Cell.* 2010;22(7):2444-58.
- 512 72. Adachi H, Contreras MP, Harant A, Wu CH, Derevnina L, Sakai T, et al. An N-terminal motif in  
513 NLR immune receptors is functionally conserved across distantly related plant species. *Elife.* 2019;8.
- 514 73. Rairdan GJ, Collier SM, Sacco MA, Baldwin TT, Boetrich T, Moffett P. The coiled-coil and  
515 nucleotide binding domains of the Potato Rx disease resistance protein function in pathogen  
516 recognition and signaling. *Plant Cell.* 2008;20(3):739-51.
- 517 74. Wu CH, Abd-El-Halim A, Bozkurt TO, Belhaj K, Terauchi R, Vossen JH, et al. NLR network  
518 mediates immunity to diverse plant pathogens. *Proc Natl Acad Sci U S A.* 2017;114(30):8113-8.
- 519 75. Castel B, Ngou PM, Cevik V, Redkar A, Kim DS, Yang Y, et al. Diverse NLR immune receptors  
520 activate defence via the RPW8-NLR NRG1. *New Phytol.* 2019;222(2):966-80.
- 521 76. Wu Z, Li M, Dong OX, Xia S, Liang W, Bao Y, et al. Differential regulation of TNL-mediated  
522 immune signaling by redundant helper CNLs. *New Phytol.* 2019;222(2):938-53.
- 523 77. Bonardi V, Tang S, Stallmann A, Roberts M, Cherkis K, Dangl JL. Expanded functions for a family  
524 of plant intracellular immune receptors beyond specific recognition of pathogen effectors. *Proc Natl*  
525 *Acad Sci U S A.* 2011;108(39):16463-8.
- 526 78. Steele JFC, Hughes RK, Banfield MJ. Structural and biochemical studies of an NB-ARC domain  
527 from a plant NLR immune receptor. *PLoS One.* 2019;14(8):e0221226.
- 528 79. Ntoukakis V, Saur IM, Conlan B, Rathjen JP. The changing of the guard: the Pto/Prf receptor  
529 complex of tomato and pathogen recognition. *Curr Opin Plant Biol.* 2014;20:69-74.
- 530 80. Gutierrez JR, Balmuth AL, Ntoukakis V, Mucyn TS, Gimenez-Ibanez S, Jones AM, et al. Prf  
531 immune complexes of tomato are oligomeric and contain multiple Pto-like kinases that diversify  
532 effector recognition. *Plant J.* 2010;61(3):507-18.
- 533 81. Mestre P, Baulcombe DC. Elicitor-mediated oligomerization of the tobacco N disease  
534 resistance protein. *Plant Cell.* 2006;18(2):491-501.

- 535 82. Zhang X, Bernoux M, Bentham AR, Newman TE, Ve T, Casey LW, et al. Multiple functional self-  
536 association interfaces in plant TIR domains. *Proc Natl Acad Sci U S A*. 2017;114(10):E2046-E52.
- 537 83. Schreiber KJ, Bentham A, Williams SJ, Kobe B, Staskawicz BJ. Multiple Domain Associations  
538 within the Arabidopsis Immune Receptor RPP1 Regulate the Activation of Programmed Cell Death.  
539 *PLoS Pathog*. 2016;12(7):e1005769.
- 540 84. Bernoux M, Ve T, Williams S, Warren C, Hatters D, Valkov E, et al. Structural and functional  
541 analysis of a plant resistance protein TIR domain reveals interfaces for self-association, signaling, and  
542 autoregulation. *Cell Host Microbe*. 2011;9(3):200-11.
- 543 85. Zhang L, Chen S, Ruan J, Wu J, Tong AB, Yin Q, et al. Cryo-EM structure of the activated NAIP2-  
544 NLRC4 inflammasome reveals nucleated polymerization. *Science*. 2015;350(6259):404-9.
- 545 86. Tentorey JL, Haloupek N, Lopez-Blanco JR, Grob P, Adamson E, Hartenian E, et al. The  
546 structural basis of flagellin detection by NAIP5: A strategy to limit pathogen immune evasion. *Science*.  
547 2017;358(6365):888-93.

## 548 Figures

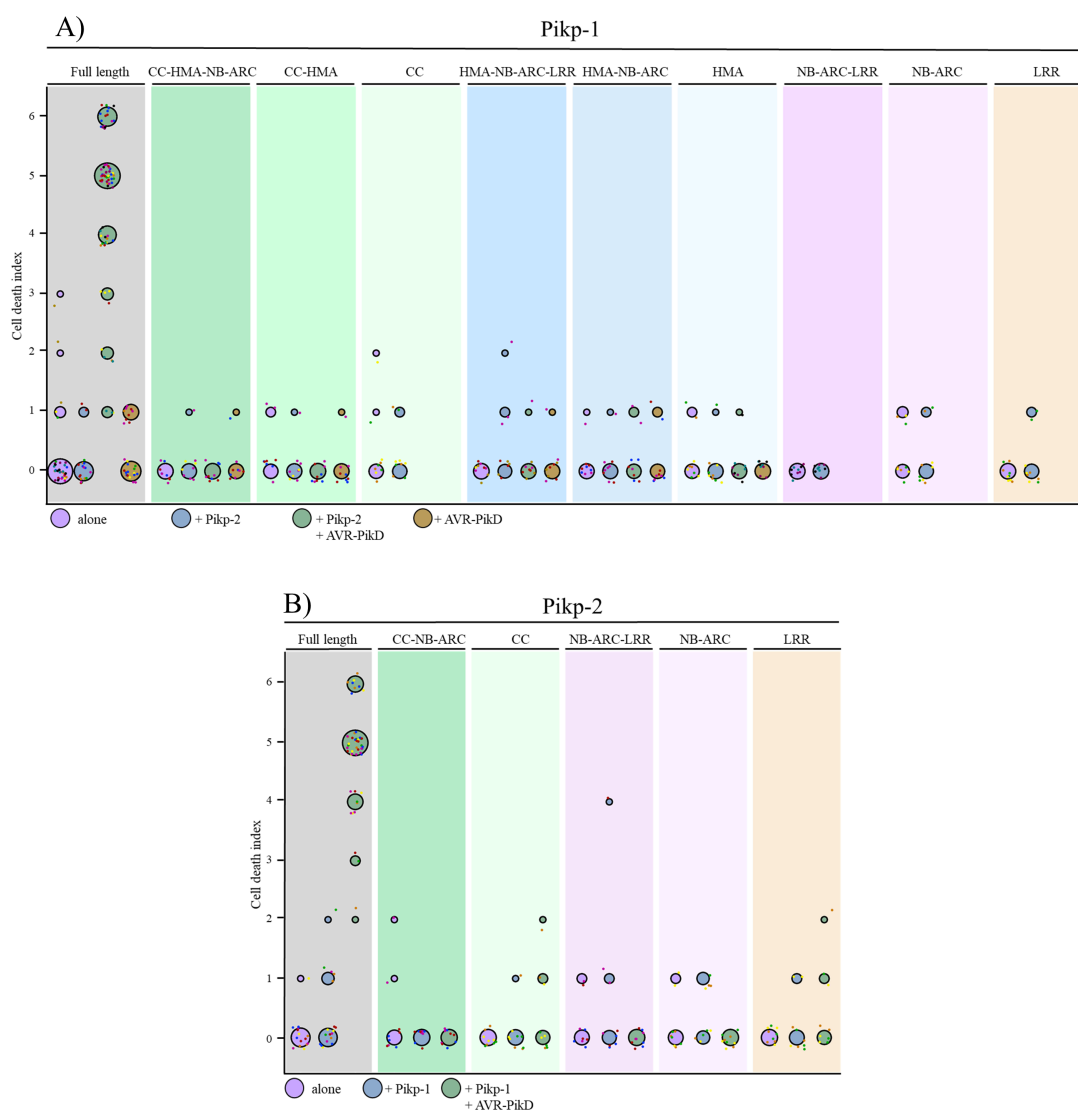


549

550 **Fig 1. Each domain of Pikp-1 and Pikp-2 is required for receptor activation. A)** Representative  
 551 *N. benthamiana* leaves showing that expression of the individual domains of Pikp-1 (left) or  
 552 Pikp-2 (right) were unable to elicit a cell death response in presence of the corresponding  
 553 paired NLR (for Pikp-1) or paired NLR and effector (for Pikp-2). Pikp-1+Pikp-2+AVR-PikD is  
 554 shown as a positive control. **B)** Representative agroinfiltration spots show that the truncated  
 555 variants of Pikp-1 (left) or Pikp-2 (right) were unable to elicit a cell death response, either  
 556 when overexpressed alone, or in the presence of corresponding full-length NLR and/or

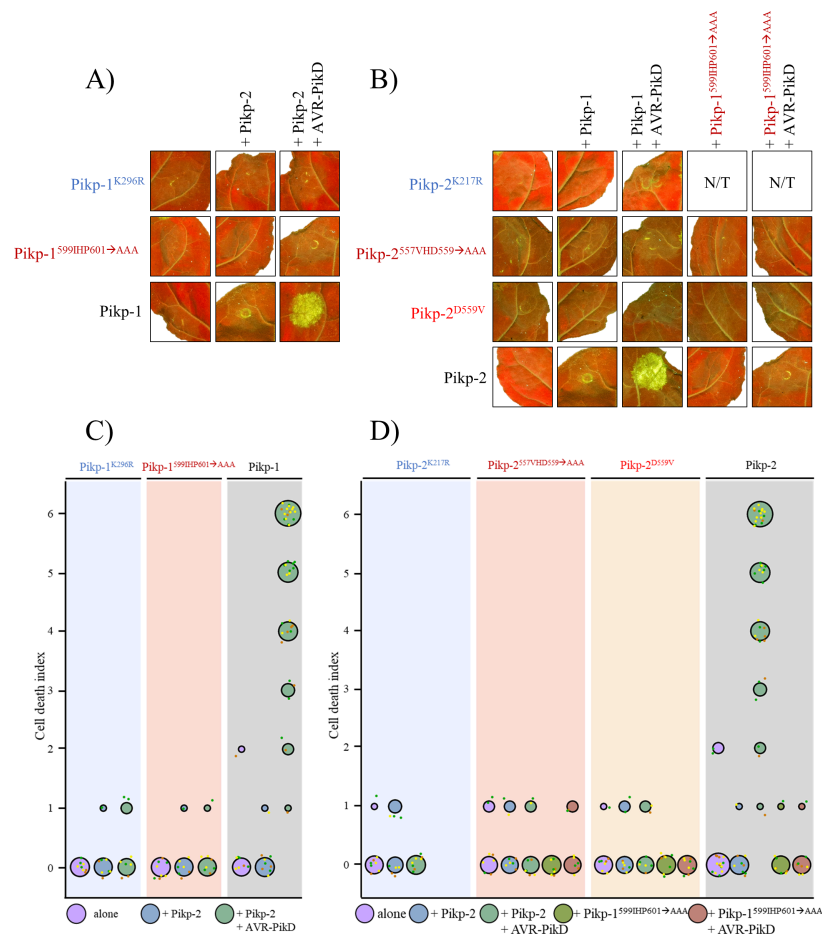
557 effector. Combinations of constructs without HMA domain were not tested (N/T) in presence  
558 of the effector.





559

560 **Fig 2. Each domain of Pikp-1 and Pikp-2 is required for receptor activation.** Cell death  
 561 quantification for the infiltration combinations of Fig 1 shown as dot plots, for Pikp-1 **(A)** and  
 562 Pikp-2 **(B)** respectively. Each of the dots has a distinct colour corresponding to the biological  
 563 replicate, and are plotted around the cell death score for visualization purposes. Each set of  
 564 infiltrations were repeated in 3 biological replicates with at least 2-3 technical replicates. The  
 565 size of the central dot at each cell death value is proportional to the number of replicates of  
 566 the sample with that score.



567

568 **Fig 3. Conserved NB-ARC domain sequence motifs are required for Pikp-1 and Pikp-2**

569 **activity. A)** Mutation of the P-loop motif of Pikp-1 ( $\text{Pikp-1}^{\text{K296R}}$ ) results in loss of cell death

570 response upon effector perception. Mutation of the Pikp-1 MHD-like motif (Pikp-

571  $1^{599\text{IHP601}\rightarrow\text{AAA}}$ ) does not lead to auto-activity when overexpressed alone, or in the presence of

572 corresponding intact NLR. Further, this mutant was also unable to trigger a cell death

573 response when co-expressed with AVR-PikD. **B)** Mutation of the P-loop motif of Pikp-

574  $2^{\text{K217R}}$ ) results in loss of cell death response upon effector perception. Mutation of the Pikp-2

575 MHD-like motif ( $\text{Pikp-2}^{557\text{VHD559}\rightarrow\text{AAA}}$  and  $\text{Pikp-2}^{\text{D559V}}$ ) does not lead to auto-activity when

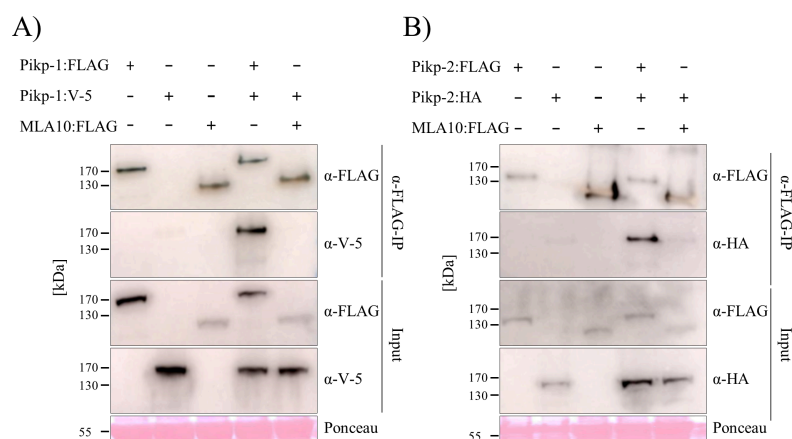
576 overexpressed alone, in the presence of corresponding intact NLR, or its MHD-like mutant.

577 Further, these mutants were also unable to trigger a cell death response when co-expressed

578 with AVR-PikD. Each set of infiltrations were repeated in 3 biological replicates with at least

579 2-3 technical replicates within each. The square showing the infiltration spot for wild type

580 Pikp-1+Pikp-2 was as-used in Fig. 1B. Squares representing Pikp-1<sup>599IHP601→AAA</sup>+Pikp-2 and  
581 Pikp-1<sup>599IHP601→AAA</sup>+Pikp-2+AVR-PikD are the same on both panels, presented for comparison.  
582 **C) and D)** Cell death quantification for each infiltration shown as dot plots. Each of the dots  
583 has a distinct colour corresponding to the biological replicate, and are plotted around the cell  
584 death score for visualization purposes. The size of the central dot at each cell death value is  
585 proportional to the number of replicates of the sample with that score. The data for Pikp-  
586 1+Pikp-2 (wild type) is a subset of the previous experiment (Fig 2A, Fig 2B), used here for  
587 comparison. The data shown for Pikp-1+Pikp-2, Pikp-1+Pikp-2+AVR-PikD, Pikp-1<sup>599IHP601</sup>+Pikp-  
588 2 and Pikp-1<sup>599IHP601</sup>+Pikp-2+AVR-PikD are the same in both panels, presented for comparison.



589

590 **Fig 4. Pikp-1 and Pikp-2 form homo-complexes. A)** Pikp-1:FLAG, Pikp-1:V-5 and MLA10:FLAG

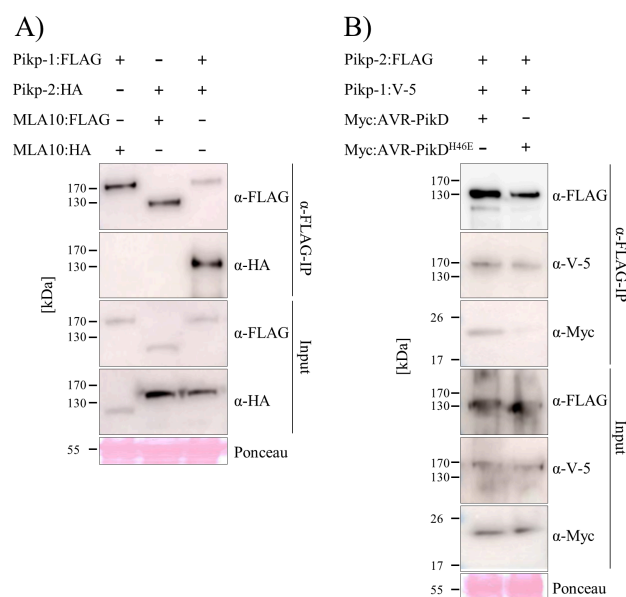
591 and **B)** Pikp-2:FLAG, Pikp-2:HA and MLA10:FLAG were expressed alone or in the combinations

592 shown. Subsequently, anti-FLAG immunoprecipitation ( $\alpha$ -FLAG-IP) was performed, followed

593 by western blot analysis with relevant antibodies to detect the proteins (upper panel). The

594 lower panel confirms presence of all the proteins prior to immunoprecipitation. Experiments

595 were repeated at least 3 times with similar results.



596

597 **Fig 5. Pikp-1 and Pikp-2 form hetero-complexes prior to and upon recognition of AVR-PikD.**

598 **A)** Pikp-1:FLAG, Pikp-2:HA, MLA10:FLAG and MLA10:HA and **B)** Pikp-2:FLAG, Pikp-1:V-5,

599 Myc:AVR-PikD and Myc:AVR-PikD<sup>H46E</sup> were expressed in the combinations shown.

600 Subsequently, anti-FLAG immunoprecipitation ( $\alpha$ -FLAG-IP) was performed, followed by

601 western blot analysis with relevant antibodies to detect the proteins (upper panel). The lower

602 panel confirms presence of all the proteins prior to immunoprecipitation. Experiments were

603 repeated at least 3 times with similar results.